

NUMERICAL STUDY OF A DESCENDING SPHERE IN A LOW REYNOLDS NUMBER STRONGLY STRATIFIED FLUID*

CARLOS R. TORRES^{†‡}, DANY DE CECCHIS^{‡§}, GERMÁN LARRAZÁBAL^{†§}, AND JOSÉ CASTILLO[§]

Dedicated to Víctor Pereyra on the occasion of his 70th birthday

Abstract. The flow generated by a sphere descending uniformly in a linearly stratified diffusive fluid is investigated numerically for different Reynolds (Re) and Froude (F) numbers. The parameters used for the simulations were $10^{-1} \leq Re \leq 10$ and $10^{-2} \leq F \leq 10^2$, keeping the Schmidt number, $Sc (= 700)$, typical of sea water) fixed. The results demonstrate drag dependence on viscosity and stratification, suggesting that changes in these parameters would be intimately related to the phenomena of zooplankton vertical movement in the ocean.

Key words. stratified fluid, flow past sphere, low Reynolds number, MAC method, preconditioning, Krylov methods.

AMS subject classifications. 35Q30, 35Q35, 35K15, 35K20

1. Introduction. Fluid flow at low Reynolds number is important in micro fluid dynamics. Applications include particle tracking in microgravity, sedimentation of particles, and motion of marine microorganisms [1, 5] among others. Due to its small size, marine microorganisms such as zooplankton are exposed to viscous fluids ($Re \ll 1$). Under these circumstances, microorganisms have to overcome physical fluid forces that could limit their ability to locate nutrient patches, mate, or escape from their predators [6, 7].

Typical oceanic conditions (viscous, density-stratified, and diffusive fluid) for microorganisms can be characterized by three non-dimensional numbers: Reynolds, $Re (= WL/\nu)$, Froude, $F (= W/NL)$, and Schmidt, $Sc (= \nu/\kappa)$, where W and L represent typical velocity and longitude, respectively; ν is the kinematic viscosity; and κ is the salt diffusivity in water. N is the Brünt–Väisälä frequency, defined as $N^2 = -g\rho_o^{-1}\partial\rho/\partial z$, where ρ_o is the reference fluid density; g , acceleration of gravity; and $\partial\rho/\partial z$, the background density gradient. The combination of these three parameters in numerical simulations allows for the study of fluid (or particle) microorganism interactions under many flow scenarios.

Due to its simplicity, a sphere is commonly used in most numerical fluid studies involving particles. Torres et al. [10] simulated the flow around a uniformly descending sphere in a density-stratified diffusive fluid within the parameter ranges $10 \leq Re \leq 200$ and $0.2 \leq F \leq 200$. Depending on the particular conditions of stratification and viscosity, a rear jet or internal waves were generated. Also, an increase on drag with stratification was shown. In the ocean, temperature (density) of the water column varies from a homogeneous to a stratified state as solar heating changes seasonally. Also, fluid flow velocity could change due to advection. Such changes in density stratification (F) or in fluid velocity (Re) could affect the motion of microorganisms (or particles) within the oceanic environment. For example, with $F = 10^3 \sim 10$, $Re = 1 \sim 10$, kinematic viscosity $\nu \sim 10^{-6} m^2/s$, vertical velocity $W \sim 10^{-3} m/s$, and stability frequency $N = 10^{-3} \sim 10^{-2} rad/s$, zooplankton with typical

*Received April 2, 2008. Accepted January 8, 2009. Published online on August 25, 2009. Recommended by Godela Scherer.

[†]Grupo de Procesos Litorales. Instituto de Investigaciones Oceanológicas. Universidad Autónoma de Baja California. A.P. 453, C.P. 22800, Ensenada, B. C. Mexico.

[‡]Multidisciplinary Center of Scientific Visualization and Computing. Faculty of Sciences and Technology. University of Carabobo. Campus Universitario, Decanato FACYT, Bárbula, Naguanagua, Venezuela. {dcecchis, glarrazal}@uc.edu.ve

[§]Computational Science Research Center. 5500 Campanile Dr. San Diego State University. San Diego, CA 92182-1245. ctorres@sciences.sdsu.edu, castillo@myth.sdsu.edu

size, $L = 10^{-3} \sim 10^{-2} m$, would be exposed to anomalously more drag than if they were in a homogeneous fluid, according to previous results [2, 10].

In this paper, in order to elucidate the dependence of drag on stratification and viscosity of particles under oceanic conditions, a series of numerical experiments for a uniformly descending sphere in a linearly stratified diffusive fluid are conducted. The range of the parameters for the simulations are $10^{-1} \leq Re \leq 10$ and $10^{-2} \leq F \leq 10^2$, keeping $Sc (= 700, \text{ typical of sea water})$ fixed. Previous numerical experiments with a similar setup were performed in the parameter ranges $10 \leq Re \leq 200$ and $0.2 \leq F \leq 200$, using traditional SOR (Successive Over-relaxation) iterative method to solve the pressure equation (2.3) [10, 11]. However, for the parameters range investigated here, an efficient implementation (see [3]) of the GMRES (Generalized Minimal RESidual) method [9], preconditioned by Incomplete LU factorization [8], was found to be superior to the SOR method used previously in [10, 11], and it was incorporated in a new code as described in [4]. The improved version has been used in even more complicated flow situations (i.e., very low $Re \sim 10^{-2}$ numbers and strong stratification) with excellent results when compared to laboratory experiments, as detailed in [12].

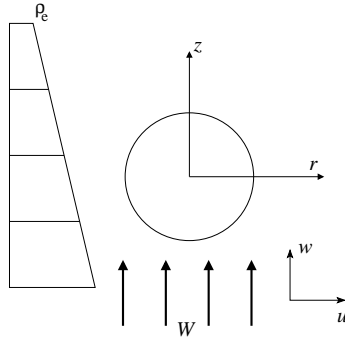


FIGURE 2.1. A sketch of the numerical problem.

2. Governing equations. We consider a sphere of radius a descending uniformly with velocity W in a linearly stratified diffusive fluid. This setup is equivalent to the case in which the sphere is fixed and the flow passes around it as shown in Figure 2.1. The set of non-dimensional perturbed equations describing this problem has been given previously [10, 11]:

$$\frac{D\mathbf{u}}{Dt} = -\nabla p - \frac{1}{F^2}\rho\mathbf{j} + \frac{2}{Re}\nabla^2\mathbf{u}, \quad (2.1)$$

$$\frac{D\rho}{Dt} = w - 1 + \frac{2}{Sc}\nabla^2\rho, \quad (2.2)$$

$$\nabla^2 p = -\frac{1}{F^2}\nabla \cdot (\rho\mathbf{j}) - \nabla \cdot [(\mathbf{u} \cdot \nabla)\mathbf{u}] + \frac{2}{Re}\nabla^2 D - \frac{\partial D}{\partial t}, \quad (2.3)$$

where $\mathbf{u} = (u, w)$ is the velocity vector, p is the pressure, ρ is the perturbed density, \mathbf{j} is the vertical unit vector, and the dimensionless numbers were defined previously. Equation (2.3) substitutes the incompressibility condition and $D(= \nabla \cdot \mathbf{u})$ represents the divergence of the

velocity. The dimensionless operators ∇^2 and ∇ are given by

$$\nabla^2 = \frac{\partial^2}{\partial z^2} + r^{-1} \frac{\partial}{\partial r} \left(r \frac{\partial}{\partial r} \right), \quad (2.4)$$

$$\nabla = \left(\frac{\partial}{\partial z} \right) \mathbf{i} + \left(\frac{\partial}{\partial r} \right) \mathbf{j}, \quad (2.5)$$

with \mathbf{i} and \mathbf{j} as the unit vectors in the z and r directions respectively in a cylindrical coordinate system [10].

The form coefficient C_p and friction coefficient C_f , from which we can calculate the drag ($C_d = C_p + C_f$), are given by

$$C_p = \frac{1}{\frac{1}{2}\rho_o W^2 \pi a^2} \int_S (-p \delta_{i,j}) \mathbf{n}_j dS, \quad (2.6)$$

$$C_f = \frac{1}{\frac{1}{2}\rho_o W^2 \pi a^2} \int_S \mu \left(\frac{\partial u_i}{\partial x_j} + \frac{\partial u_j}{\partial x_i} \right) \mathbf{n}_j dS, \quad (2.7)$$

where \mathbf{n}_j is the component of the unit vector normal to the sphere surface S and dS is the area element in the surface integral.

The set of equations (2.1)-(2.3) are transformed to curvilinear coordinates and solved subject to initial and boundary conditions using the finite-difference method. The boundary conditions are as follows: on solid boundaries the non-slip condition ($\mathbf{u} = 0$) is used; and at the rear boundary, the flow is allowed to leave the computational domain and the condition $\partial \mathbf{u} / \partial z = 0$ is imposed. The boundary condition for the pressure is obtained from (2.1) by setting the velocities to zero [10]. Far from the sphere $\rho \rightarrow 0$, while on the sphere surface, the no density flux condition is enforced, i.e.,

$$\frac{\partial \rho}{\partial z} z + \frac{\partial \rho}{\partial r} r = z.$$

The external boundary of the grid is elliptic with a size of 40 sphere diameters in the vertical direction and 20 sphere diameters in the horizontal direction. The grid consists of 195×91 ($\xi \times \eta$) mesh points in the (z, r) -space, with clustering of grid points on the sphere surface ($\eta = 1$) in such a way that the difference between grid point 24 ($\eta = 24$) and grid point 1 is 1×10^{-3} . For $Re = 200$ and $Sc = 700$ the thickness of the boundary layer is $\delta = 2.7 \times 10^{-3}$, while for $Re = 1$, $\delta = 0.0378$. Therefore, at least 20 grid points are available to resolve δ for $Re = 200$ and more than 20 for $Re = 1$. The smallest mesh size used is 1×10^{-5} . Figure 2.2 shows the grid near the sphere in physical space.

The simulations are performed under different flow scenarios ($10^{-1} < Re < 10$; $10^{-2} \leq F \leq 10^2$ and $Sc = 700$) using an improved version [4] of a previous code [10]. The tolerance to attain the steady state solution for velocities and density calculations is set to 10^{-4} , while the pressure tolerance is set to 10^{-13} . Typical time step for simulations are $\Delta t = 0.0025$ or $\Delta t = 10^{-4}$. Nearly steady states are reached at dimensionless time $t \sim 30$.

3. Discussion. Figure 3.1 depicts the change of flow pattern with Reynolds number as the sphere descends in a slightly stratified fluid ($F = 200$). It is observed that there is no rear vortex (Figure 3.1a) and the isopycnals tend to open far from the sphere surface. This effect could be linked to the thickening of the boundary layer (δ) with increasing viscosity ($Re \rightarrow 0$), which for the Reynolds number of Figure 3.1 (i.e., $Re = 0.8, 0.4$, and 0.2) is $\delta = 0.0423, 0.0598$, and 0.0845 , respectively.

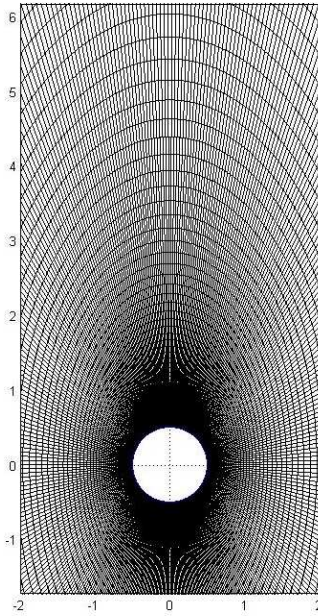


FIGURE 2.2. The grid near the sphere in physical space.

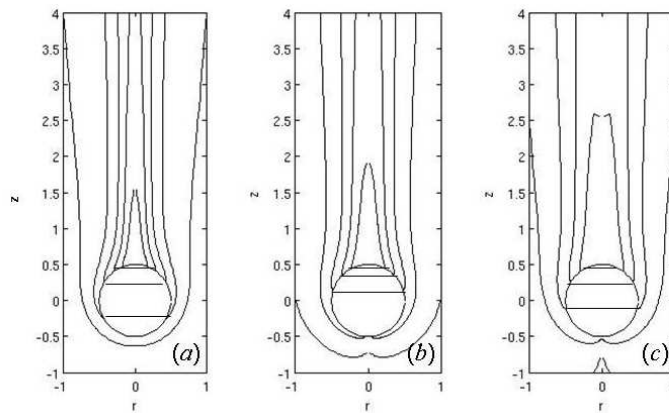


FIGURE 3.1. Isopycnals for $F = 200$ and various Re numbers. Contours are drawn for $\rho - z = 0, -2, -4, -6$. a) $Re = 0.8$, b) $Re = 0.4$, c) $Re = 0.2$.

Figure 3.2 shows the typical change of flow pattern with stratification at low Reynolds number ($Re = 1$). It is observed that the density surfaces tend to embrace the sphere as stratification becomes stronger ($F \rightarrow 0$, Figures 3.2b and 3.2c). When stratification is very weak ($F = 200$, Figure 3.2a), the flow pattern is almost identical to that of homogeneous fluid, and the drag coefficient agrees very well with those reported in the literature.

Figures 3.1 and 3.2 also show that a number of density contours disappear on the sphere surface. That is a result of the addition of diffusion in the density boundary layer (equation (2.2)), which prevents isopycnals from piling up in front of the sphere. This mechanism was

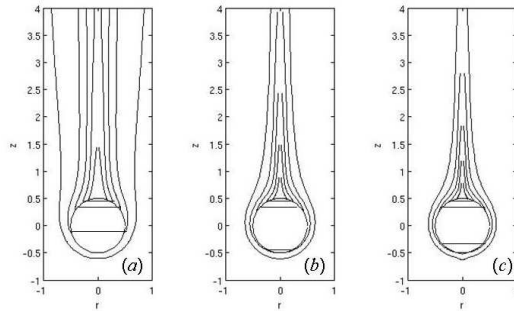


FIGURE 3.2. *Isopycnals for $Re = 1$ and various F numbers. Contours are drawn for $\rho - z = 0, -2, -4, -6$. a) $F = 200$, b) $F = 1$, c) $F = 0.6$.*

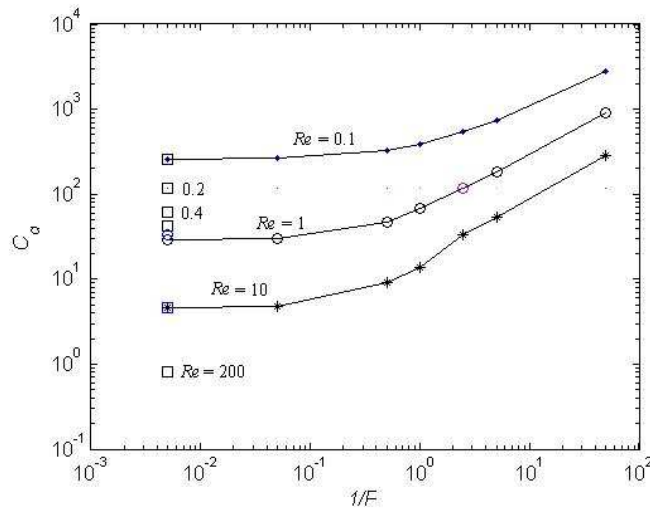


FIGURE 3.3. *Dependence of total drag coefficient C_d on Re and $1/F$. Unstratified C_d values for other Re numbers (small boxes) are included for reference.*

discussed in detail in [10].

The dependence of C_d on the Reynolds and the inverse of the Froude number are shown in Figure 3.3. There is an increasing total drag (C_d) with increasing stratification ($F \rightarrow 0$) and viscosity ($Re \rightarrow 0$). For example, $C_d = 4.54$ ($Re = 10$), which is about five times larger than $C_d = 0.8$ of the unstratified total drag for $Re = 200$. The mechanisms of drag increase at these flow conditions have been attributed to the rearward movement of the separation point and the subsequent change in the pressure and shear stress distributions, as discussed in Torres et al. [10]. A comparison of the values of the C_p and C_f coefficients in this study shows that more of the total drag coefficient (C_d) comes from C_f than from C_p .

The rapid increase of drag for $F > 1$ may be important for small organisms such as zooplankton with regard to searching for food or escaping from their predators. Under strong

stratification conditions, such microorganisms could expend much more of their energy to reach patches of food than they would under conditions of no stratification.

4. Conclusions. A numerical study is performed of a low Reynolds number strongly stratified fluid moving past a sphere. The results show that at low Reynolds numbers, drag increases as stratification becomes stronger. It appears that there is no separation of the flow as indicated by the density surface plots but a more detailed study is suggested. Application of these results to motion of very small organisms, such as zooplankton, could be important when considering the energy they expend in search of food sources or maintaining their position within the fluid.

Acknowledgments. This work was sponsored by *Consejo de Desarrollo Científico y Humanístico* (CDCH), Universidad de Carabobo under Project *Partícula-pared para número de Reynolds bajo usando la biblioteca UCSparseLib*.

REFERENCES

- [1] F. AZAM AND F. MALFATTI, *Microbial structuring of marine ecosystems*, Nature Reviews Microbiology, 5 (2001), pp. 782–791.
- [2] H. HANAZAKI, K. KONISHI, AND T. OKAMURA, *Schmidt-number effects on the flow past a sphere moving vertically in a stratified diffusive fluid*, Phys. Fluids, 21 (2009), pp. 1–8.
- [3] G. LARRAZÁBAL, *UCSparseLib: A numerical library to solve sparse linear systems*, in Numerical Simulation and Computational Modeling, V. Rogo, M. J. Torres, and M. Cerrolaza, eds., SVMNI, 2004, pp. TC19–TC25.
- [4] G. LARRAZÁBAL, C. R. TORRES, AND J. CASTILLO, *An efficient and robust algorithm for 2D stratified fluid flow calculations*, Appl. Num. Math., 47 (2003), pp. 493–502.
- [5] A. G. LEWIS, S. E. ALLEN, AND G. MARTENS, *Rapid swimming and the median intersomitic ridge in calanoid copepods*, Crustaceana, 79 (2006), pp. 501–511.
- [6] R. LIEBE, *Flow Phenomena in Nature: A Challenge to Engineering Design*, vol. 7 of Design and Nature, WIT Press, Billerica, Massachusetts, 2006.
- [7] MARCOS AND R. STOCKER, *Microorganisms in vortices: a microfluidic setup*, Limnol. Oceanogr: Methods, 4 (2006), pp. 392–398.
- [8] Y. SAAD, *ILUT: A dual threshold incomplete LU factorization*, Numer. Linear Algebra Appl., 1 (1994), pp. 387–402.
- [9] ———, *Iterative Methods for Sparse Linear Systems*, 2nd ed., SIAM, Philadelphia, 2003.
- [10] C. R. TORRES, H. HANAZAKI, J. OCHOA, J. CASTILLO, AND M. VAN WOERT, *Flow past a sphere moving vertically in a stratified diffusive fluid*, J. Fluid Mech., 417 (2000), pp. 211–236.
- [11] C. R. TORRES, J. OCHOA, J. CASTILLO, AND M. VAN WOERT, *Initial flow field of stratified flow past an impulsively started sphere*, Appl. Numer. Math., 40 (2002), pp. 235–244.
- [12] K. YICK, C. R. TORRES, T. PEACKOCK, AND R. STOCKER, *Enhanced drag of a sphere settling in a stratified fluid at small Reynolds numbers*, J. Fluid Mech., 632 (2009), pp. 49–68.